

MicroRNA-421 regulated by HIF-1 α promotes metastasis, inhibits apoptosis, and induces cisplatin resistance by targeting E-cadherin and caspase-3 in gastric cancer

Xiaoxiao Ge^{1,2,*}, Xinyang Liu^{3,4,*}, Fengjuan Lin^{1,2,*}, Peng Li⁴, Kaiyi Liu^{1,2}, Ruixuan Geng⁶, Congqi Dai^{1,2}, Ying Lin^{1,2}, Wenbo Tang^{1,2}, Zheng Wu^{1,2}, Jinjia Chang^{1,2}, Jianwei Lu⁷, Jin Li^{1,2}

¹Department of Medical Oncology, Fudan University, Shanghai Cancer Center, Shanghai, 200000, P.R. China

²Department of Oncology, Shanghai Medical College, Fudan University, Shanghai, 200000, P.R. China

³Shanghai Medical College, Fudan University, Shanghai, 200000, P.R. China

⁴Harvard T.H. Chan School of Public Health, Boston, MA, 02115, U.S.A

⁵Department of Regenerative Medicine and Stem Cell Research Center, Tongji University School of Medicine, Shanghai, 20000, P.R. China

⁶International Medical Services, Peking Union Medical College Hospital, Beijing, 100000, P.R. China

⁷The Advanced Institute of Translational Medicine and School of Software Engineering, Tongji University, Shanghai, 200073, P.R. China

*These authors have contributed equally to this work

Correspondence to: Jin Li, e-mail: fudanlijin@163.com
Jianwei Lu, e-mail: jianweilu_tongji@sina.com

Keywords: gastric cancer, miR-421, HIF-1 α , cisplatin resistance, epithelial-mesenchymal transition

Received: November 25, 2015

Accepted: March 01, 2016

Published: March 21, 2016

ABSTRACT

Hypoxia and dysregulation of microRNAs (miRNAs) have been identified as crucial factors in carcinogenesis. However, the potential mechanisms of HIF-1 α and miR-421 in gastric cancer have not been well elucidated. In this study, we found that miR-421 was up-regulated by HIF-1 α . Overexpression of miR-421 promoted metastasis, inhibited apoptosis, and induced cisplatin resistance in gastric cancer *in vivo* and *in vitro*. E-cadherin and caspase-3 were identified as targets of miR-421. Besides, relative mRNA expression of miR-421 was significantly increased in gastric cancer tumor tissues compared with non-tumor tissues in a cohort of gastric cancer specimens (n=107). The expression of miR-421 was higher in advanced gastric cancers compared with localized ones. Moreover, Kaplan–Meier analysis illustrated that those patients with low levels of miR-421 had a significant longer overall survival (p = 0.006) and time to relapse (p = 0.007). Therefore, miR-421 could serve as an important prognostic marker and a potential molecular target for therapy in gastric cancer.

INTRODUCTION

Hypoxia, a common feature of rapidly growing tumors, is associated with various physiological and pathophysiological events, including carcinogenesis, cancer cell migration and invasion, angiogenesis and chemotherapy resistance [1, 2]. These changes are regulated by a series of hypoxia-induced genes [3]. HIF-1 α , induced by hypoxia, is regarded as the key transcription factor in downstream regulation [3], and activates a signaling transduction

network including cell cycle, cell apoptosis and metastasis which drives the adaptation of cancer cells under hypoxic conditions to a more aggressive phenotype [4]. Previous studies illustrated the correlation between drug resistance and epithelial-mesenchymal transition (EMT), and indicated that EMT played a critical role in chemotherapy resistance [5–7]. Moreover, inhibition of cell apoptosis was another important process in decreasing the chemotherapy sensitivity [8]. However, the correlation among HIF-1 α , EMT, and apoptosis and its underlying mechanisms in regulation of chemotherapy resistance have not been well elucidated.

microRNAs (miRNAs) are evolutionally conserved, endogenous, non-coding, small (20–23 nucleotides) RNAs, which regulate gene expression at post transcriptional level [9]. miRNAs accelerate the degradation and/or block the translation of their target mRNAs to induce post-transcriptional gene repression, and regulate various cellular processes such as proliferation, differentiation, metabolism and apoptosis [10]. Loss expression of miRNA genes was firstly observed in leukemia, and demonstrated the critical role of miRNAs in carcinogenesis [11]. Subsequent researches illustrated the carcinogenesis of miRNAs in many types of cancer [7, 12–14].

Recent researches illustrated that hypoxia regulated a series of miRNAs, which coordinated with HIF-1 α to modulate cell proliferation, metastasis, apoptosis and angiogenesis [8, 15–17]. miR-210, a classic HIF-1 α induced miRNA, has been reported to be involved in many aspects of carcinogenesis [18]. HIF-1 α induced miR-382 has also been reported as an angiogenic miRNA by suppressing the expression of PTEN [15]. Recently, miR-421 has been found to be able to promote cell proliferation and migration in hepatocellular carcinoma, nasopharyngeal carcinoma, and neuroblastoma [19–21]. However, little is known about its role under hypoxia in gastric cancer.

Therefore, in our study, we investigated the roles of HIF-1 α induced miR-421 in gastric cancer, and we found that miR-421 promoted metastasis, inhibited apoptosis, and induced cisplatin resistance by targeting E-cadherin and caspase-3.

RESULTS

Elevated HIF-1 α induces cisplatin resistance in gastric cancer

In order to verify the change of HIF-1 α under hypoxia in gastric cell lines, we used cobalt chloride (CoCl₂) and Dimethylxalylglycine (DMOG) to simulate the hypoxia environment. The SGC-7901 and AGS gastric cancer cell lines were treated from 0h to 48h with the hypoxia mimetic agent CoCl₂ (100 μ M). The expression of HIF-1 α increased in both cell lines and reached the highest point at 24h (Figure 1A). Next, we used CoCl₂ and DMOG (300 μ M) to treat both cell lines for 24h. The result indicated that CoCl₂ made the protein level of HIF-1 α more stable in gastric cell lines compared to DMOG (Figure 1B). To further testify the function of HIF-1 α , we co-transfected Si-HIF-1 α (50 μ M) with CoCl₂ to detect the expression of HIF-1 α , and we found that Si-HIF-1 α could reverse the stabilized effect of CoCl₂ on HIF-1 α in both cell lines (Figure 1C). Therefore, we chose CoCl₂ for the follow-up experiments.

To explore the biological function of HIF-1 α in gastric cancer, cisplatin-induced anti-cancer function was analyzed in SGC-7901 and AGS gastric cancer cell lines under hypoxia. The IC₅₀ of cisplatin in SGC-7901 and

AGS gastric cancer cell lines were 2.4 \pm 0.66 μ M and 20.8 \pm 4.50 μ M. After treated with CoCl₂ for 24h, the IC₅₀ of cisplatin in both cell lines increased to 72.1 \pm 5.20 μ M and 82.3 \pm 4.70 μ M, respectively (Figure 2A).

Flow cytometry was conducted to determine whether cisplatin induced apoptosis was affected by hypoxia. The gastric cell lines treated with DMSO, the solvent of cisplatin, were used as controls. Flow cytometry analysis indicated that cisplatin drastically increased the percentage of early apoptotic cells in both cell lines. The apoptotic ability was attenuated by induction of CoCl₂ (Figure 2B). Furthermore, CoCl₂ increased the colony forming ability in cisplatin treated gastric cell lines. Compared with cell lines treated cisplatin alone, the colony formation ability increased drastically in cisplatin and CoCl₂ group (Figure 2C). Besides, western blotting analysis indicated that cisplatin significantly elevated the expression of cleaved caspase-3 and cleaved PARP, which could be reversed by induction of CoCl₂, indicating that CoCl₂-induced HIF-1 α suppressed the cisplatin-induced apoptosis (Figure 2E).

To further elucidate the function of HIF-1 α in gastric cancer, we investigated the effect of CoCl₂ on cisplatin-treated SGC-7901 and AGS cell motility via transwell assay. The results suggested that cisplatin decreased the migration and invasion ability of both cell lines, and the inhibitory effect could be reversed by induction of CoCl₂ (Figure 2D). EMT is an important process in invasion and metastasis of cancer and the loss expression of E-cadherin is a key factor in EMT. Western blotting was used to analyze the expression of EMT-related proteins in cisplatin-treated cell lines treated with CoCl₂. As a result, the expression of E-cadherin was increased, and that of N-cadherin, Fibronectin, Vimentin and Snail was decreased by cisplatin. However, the increased expression of E-cadherin and the decreased expression of N-cadherin, Fibronectin, Vimentin and Snail were attenuated by induction of CoCl₂ in both cell lines (Figure 2E). Besides, we also found that the epithelial biomarker E-cadherin was significantly down regulated, whereas the mesenchymal biomarkers N-cadherin, Fibronectin, Vimentin and Snail were up regulated when treated with CoCl₂ alone (Figure 2E).

HIF-1 α is involved in miR-421 expression

To explore the change of miRNA in gastric cancer cells under hypoxic conditions, a miRNA microchip was used in a previous study [15]. As a result, 43 miRNAs were up regulated by over 2-fold, whereas 12 miRNAs were down regulated by over 2-fold under hypoxic conditions (GSE 56870). Therefore, we used quantitative real-time PCR (qRT-PCR) to confirm the microchip data, and miR-421, miR-130b, miR-129-3p, miR-210, miR-424 and miR-382 were found to be drastically up regulated by treated with CoCl₂ and DMOG for 24h (Figure 3A). The role of hypoxia-induced miR-421 in cancer progression and drug resistance has not been elucidated in gastric

cancer. Therefore, we chose miR-421 as a candidate miRNA in regulation of drug resistance for further study.

Next, we explored the function of HIF-1 α in expression of miR-421 under hypoxic conditions. Induction of CoCl₂ up regulated the expression of endogenous miR-421, while co-transfection of HIF-1 α siRNA would down regulate the expression of miR-421 in turn in SGC-7901 and AGS gastric cancer cell lines

(Figure 3B). To further investigate regulation of miR-421 by HIF-1 α , we used the miRStart database (<http://mirstart.mbc.nctu.edu.tw/home.php>) to predict the transcription start site (TSS) of miR-421. The result indicated the TSS of miR-421 located 20170 upstream of the precursor. We used JASPAR database (<http://jaspar.genereg.net>) to predict the conserved HIF-1 α binding sequence (Hypoxia Response Element, HRE) in the promoter region of miR-

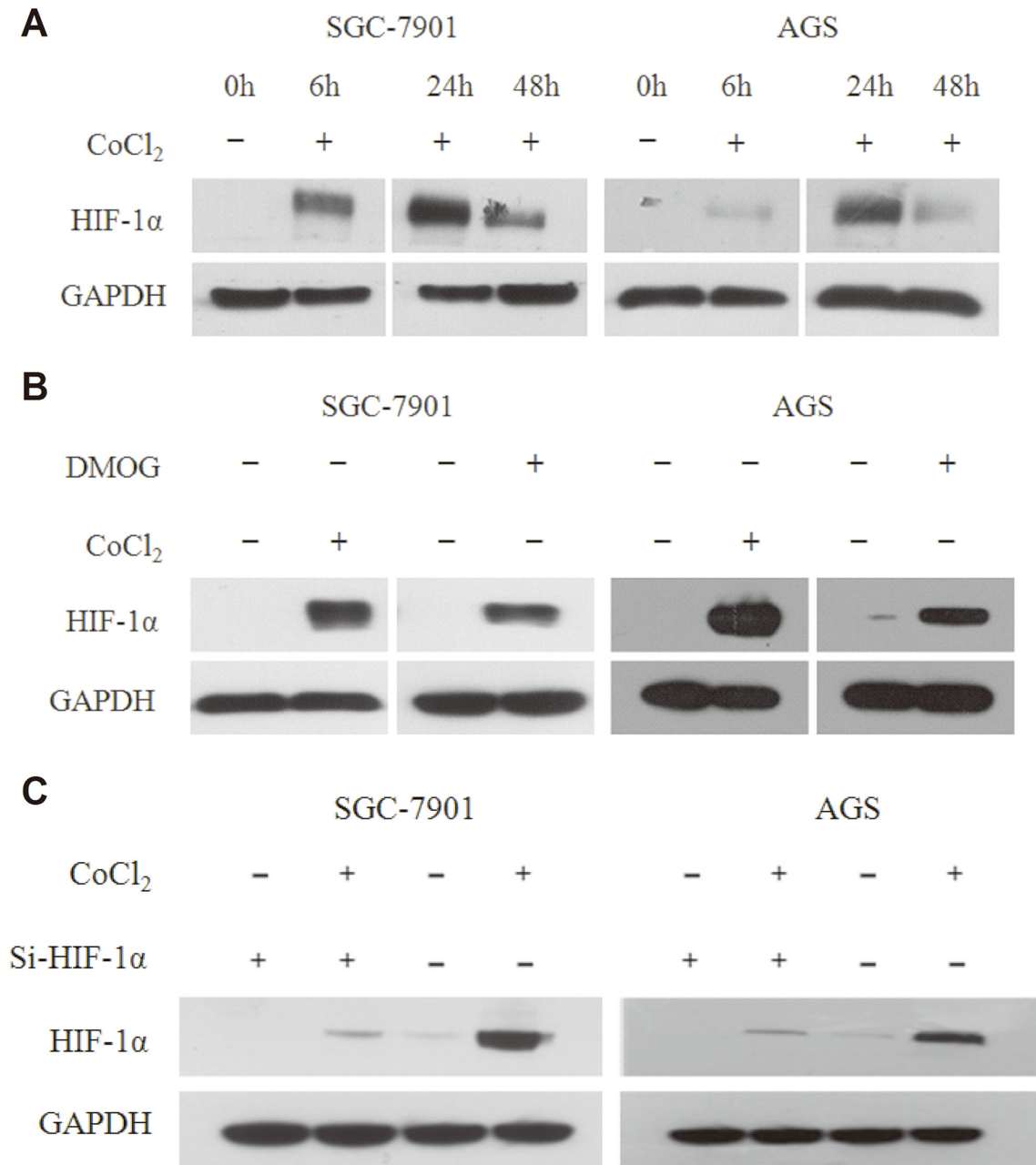


Figure 1: HIF-1 α expression is stabilized by CoCl₂ and DMOG. **A.** The expression of HIF-1 α increases in SGC-7901 and AGS gastric cancer cell lines, which were treated with the hypoxia mimetic agent CoCl₂ (100 μ M) from 0h to 48h, and reaches the highest point at 24h. **B.** Western blot analysis indicates that CoCl₂ makes the expression of HIF-1 α more stable in gastric cell lines compared to DMOG. Both cell lines were treated with CoCl₂ and DMOG (300 μ M) for 24h. **C.** Western blot analysis indicates that co-transfected Si-HIF-1 α (50 μ M) with CoCl₂ could reverse the stabilized effect of CoCl₂ on HIF-1 α in both cell lines.

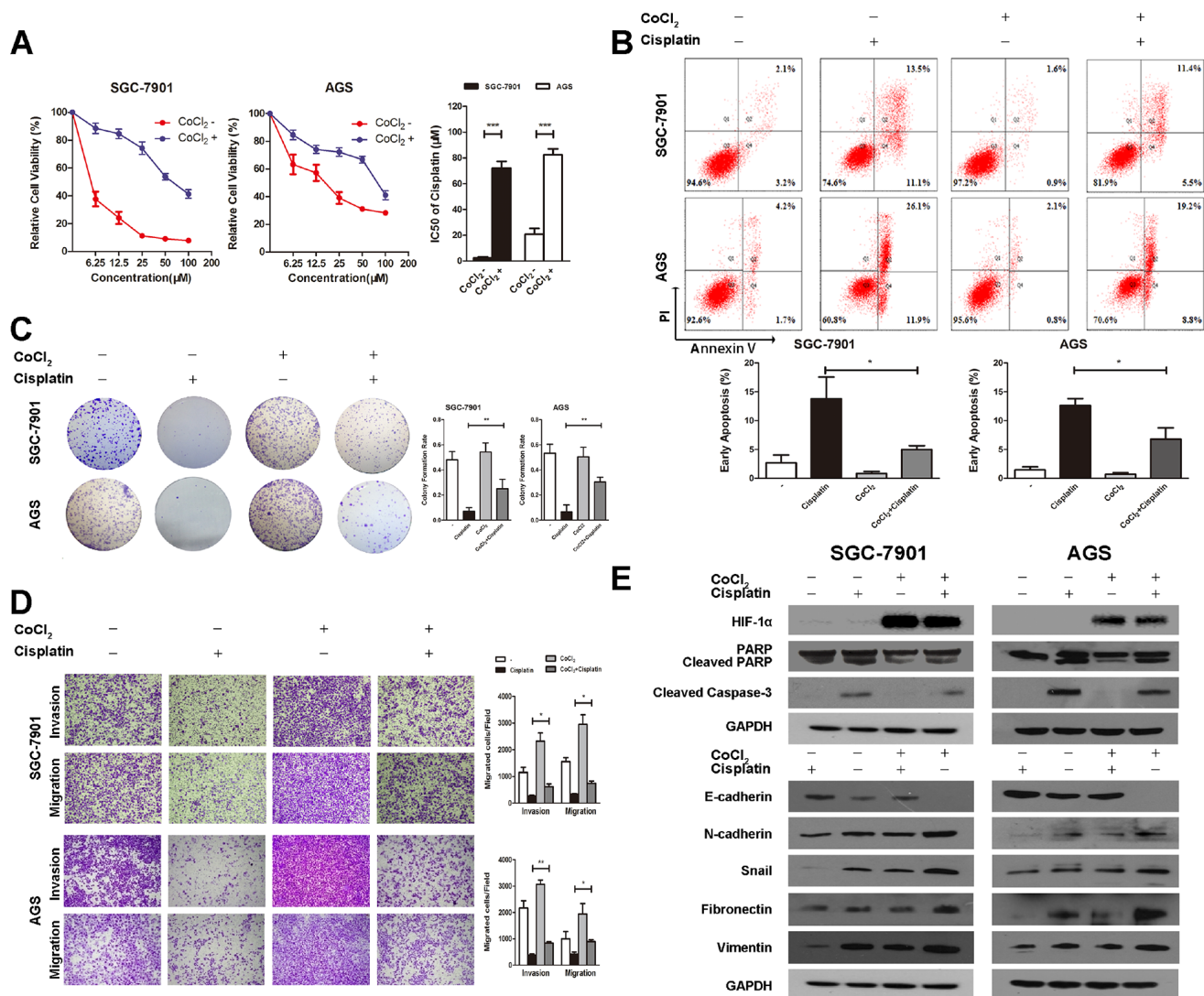


Figure 2: Elevated HIF-1 α induces cisplatin resistance in gastric cancer. **A.** The IC₅₀ of cisplatin in SGC-7901 and AGS is $2.4 \pm 0.66 \mu\text{M}$ and $20.8 \pm 4.50 \mu\text{M}$ respectively. After being treated with CoCl₂ for 24h, the IC₅₀ of cisplatin in SGC-7901 increases to $72.1 \pm 5.20 \mu\text{M}$, and AGS to $82.3 \pm 4.70 \mu\text{M}$. Error bars mean 95 % confidence intervals. Columns mean of three independent experiments, and bars SD. **B.** Flow cytometry analysis indicates that cisplatin drastically increases the percentage of early apoptotic cells in both cell lines, which could be attenuated by induction of CoCl₂. Representative images and quantitative analysis of cell apoptosis are presented. Columns mean of three independent experiments, and bars SD. **C.** CoCl₂ increases the colony forming ability in cisplatin treated gastric cell lines compared with those treated with cisplatin alone. Representative images and quantitative analysis of colony formation rate are presented. Columns mean of three independent experiments, and bars SD. **D.** Transwell assays illustrate that cisplatin decreases the migration and invasion ability of both cell lines, and the inhibitory effect could be reversed by induction of CoCl₂. Representative migration and invasion images at $\times 100$, and quantitative analysis of transwell assays are presented. Columns mean of three independent experiments, and bars SD. **E.** Western blot analysis shows that the expression of HIF-1 α is significantly increased by CoCl₂. The expression of cleaved caspase-3 and cleaved PARP are induced by cisplatin, E-cadherin is increased, and N-cadherin, Fibronectin, Vimentin, and Snail are decreased by cisplatin, which could be reversed by CoCl₂ in both cell lines. The E-cadherin is significantly down regulated, whereas N-cadherin, Fibronectin, Vimentin, and Snail are up regulated when treated with CoCl₂ alone. * $P < 0.05$; ** $P < 0.01$; *** $P < 0.001$.

421, and HIF-1 α was found to be bound to HRE in the 1 kb upstream of the TSS of miR-421. Therefore, we cloned the promoter region of miR-421 (-1 kb) harboring predicted HRE sequences into pGL3 vector. As a result, treating with CoCl₂ in HEK293T cells increased the luciferase activity of miR-421 promoter. When HEK293T

cells were co-transfected with Si-HIF-1 α , the increased luciferase activity would be diminished (Figure 3C).

Moreover, we treated gastric cancer cell line SGC-7901 xenografted male BALB/c-nude mice (4 weeks old) with BAY 87-2243, a HIF-1 α specific inhibitor, for 15 days. We used qRT-PCR to confirm that BAY 87-2243

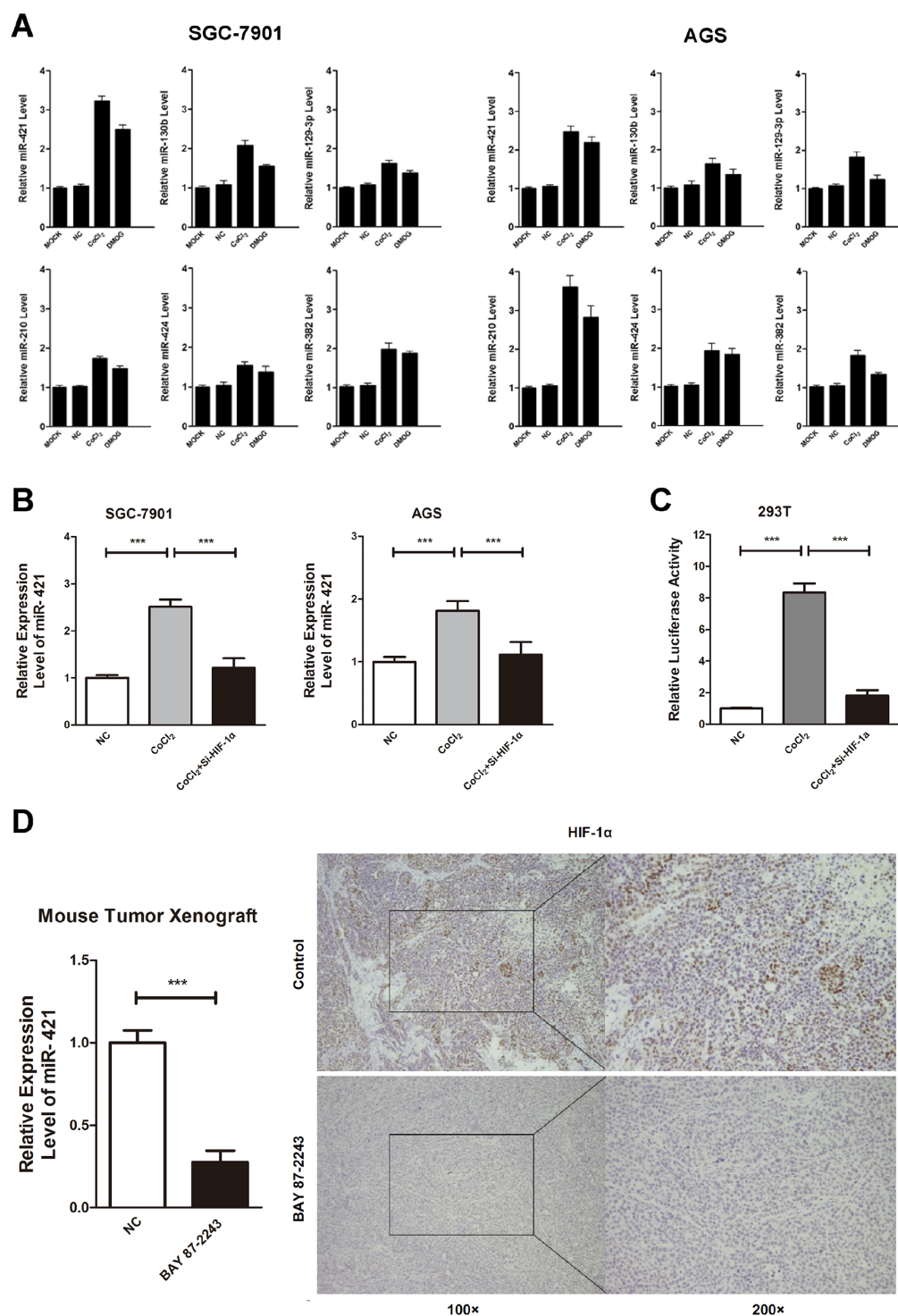


Figure 3: HIF-1 α is involved in miR-421 expression. A. Quantitative real-time PCR (qRT-PCR) was conducted to confirm the microchip data, and miR-421, miR-130b, miR-129-3p, miR-210, miR-424 and miR-382 were drastically up regulated after being treated with CoCl₂ or DMOG for 24h. Columns mean of three independent experiments. B. Induction of CoCl₂ increases the expression of endogenous miR-421, while co-transfection of HIF-1 α siRNA decreases the expression of miR-421 in SGC-7901 and AGS. Columns mean of three independent experiments. C. Induction of CoCl₂ in HEK293T cells increases the luciferase activity of miR-421 promoter. When 293T cells are co-transfected with Si-HIF-1 α , the increased luciferase activity is diminished. Columns mean of three independent experiments. D. SGC-7901 xenografted male BALB/c-nude mice (4 weeks old) were treated with BAY 87-2243, a HIF-1 α specific inhibitor, for 15 days. QRT-PCR illustrates that BAY 87-2243 reduces the expression of miR-421 by 0.27-fold in gastric cancer tissues. IHC staining confirms that the expression of HIF-1 α decreases in BAY 87-2243 treated cancer tissues compared to control group. Columns mean of three independent experiments. *** $P < 0.001$.

reduced the expression of miR-421 by 0.27-fold in gastric cancer tissues (Figure 3D). We also used IHC staining to confirm that the expression of HIF-1 α decreased in BAY 87-2243 treated cancer tissues compared to control group (Figure 3D).

Epigenetic change also plays an important role in regulation of gene expression. To clarify the potential role of epigenetic regulation of miR-421, SGC-7901 and AGS gastric cancer cell lines were treated with 5-Aza, a methyltransferase inhibitor. We found that the expression of miR-421 was significantly increased in both 5-Aza treated cell lines, suggesting existence of methylation regulation in miR-421 (Supplementary Figure S1A). Next, we used the CpG Island Searcher Program (<http://www.urogene.org/methprimer>) to identify a CpG island located 6-9 kb upstream of TSS of miR-421, and we conducted sodium bisulfite sequencing assay to assess the methylation status of the predicted CpG island (Supplementary Figure S1B). As a result, the methylation status was drastically increased in SGC-7901 and AGS gastric cancer cell lines. A total of 97.0% and 77.0% of CpGs were methylated in SGC-7901 and AGS cell lines, which further verified the involvement of methylation regulation in miR-421 silencing (Supplementary Figure S1C). Moreover, involvement of CoCl₂ increased the expression of DNA methyltransferase 1 and DNA methyltransferase 3a in both cell lines, which could further elevate the methylation level of CpG island of miR-421 and decrease the expression of miR-421 (Supplementary Figure S1D). However, as we mentioned before, miR-421 could be significantly increased in gastric cancer cell lines by treated with CoCl₂, which was contradicted with the methylation status of miR-421. Therefore, we deduced that HIF-1 α was a more powerful factor in miR-421 activation.

To further confirm the regulatory role of HIF-1 α in miR-421 activation, flow cytometry and transwell assays were conducted. We assessed the function via. Inhibitor of miR-421 reverses the function of HIF-1 α . The results indicated that CoCl₂ or miR-421 drastically decrease the percentage of apoptotic cells and increase the migration and invasion ability in cisplatin treated SGC-7901 and AGS cells, which could be reversed by transfection of miRNA-421 inhibitor (miR-421-Inh) together with CoCl₂ (Supplementary Figure S2). These results indicated that HIF-1 α is a key factor in regulation of miR-421.

MiR-421 could be a prognostic marker in gastric cancer

To investigate the potential role of miR-421 in gastric cancer, the miR-421 expression pattern was evaluated using data from The Cancer Genome Atlas (TCGA). The results showed that the relative mRNA expression of miR-421 was significantly increased in gastric cancer tumor tissues compared with non-tumor tissues in a cohort of 38 gastric cancer patients (Figure 4A).

Next, we determined the clinical significance of miR-421 by analyzing its expression pattern in 107 pairs of gastric cancer tissues and para-cancerous tissues via qRT-PCR to further confirm the finding from TCGA (Table 1). As a result, the expression of miR-421 was significantly increased in gastric cancer tissues ($p < 0.001$) (Figure 4B). In addition, we compared the expression pattern of miR-421 between localized gastric cancer and advanced gastric cancer, and the result indicated that the expression of miR-421 was higher in advanced gastric cancer compared with localized gastric cancer ($p < 0.05$), indicating miR-421 could be related to cancer aggressiveness and poor prognosis (Figure 4C). Furthermore, Kaplan–Meier analysis illustrated that those patients with low levels of miR-421 had a much longer overall survival (53.8 vs. 32.1 months, $p = 0.006$) and time to relapse (48.4 vs. 27.0 months, $p = 0.007$) (Figure 4D, 4E). Cox multivariate analysis illustrated that miR-421 was an independent predictor of overall survival ($p = 0.016$, HR 2.586, 95%CI 1.194-5.599) and recurrence-free survival ($p = 0.014$, HR 2.465, 95%CI 1.201-5.060) (Table 2). These results indicated that miR-421 was an important prognosis marker in gastric cancer. The expression of miR-421 varied dramatically among gastric cancer cell lines. The immortalized human gastric epithelial cell line GES-1 showed relatively low expression of miR-421.

Overexpression of miR-421 promotes tumor malignant behavior in gastric cancer

To understand the potential role of miR-421 in regulation of drug resistance in gastric cancer, miR-421 was transfected in cisplatin treated SGC-7901 and AGS gastric cancer cell lines to evaluate its function. To assess whether cisplatin induced apoptosis was affected by miR-421, we assessed the function via flow cytometry. The gastric cell lines treated with NC were used as controls. Flow cytometry analysis indicated that cisplatin drastically increased the percentage of early apoptotic cells in both cell lines. The apoptotic ability was attenuated by transfection of miR-421 (Figure 5A). Besides, western blotting analysis indicated that cisplatin significantly induced the activation of caspase-3 and cleavage of PARP, which could be reversed by transfection of miR-421. On the contrary, CoCl₂ induced low level of activated caspase-3 and cleavage of PARP could be reversed by transfection of miR-421-Inh (Figure 5C).

To further elucidate the function of miR-421 in gastric cancer, we investigated the effect of miR-421 on cisplatin-treated SGC-7901 and AGS cell motility via transwell assay. The results suggested that cisplatin decreased the migration and invasion ability in both cell lines, and the inhibitory effect could be reversed by transfection of miR-421 (Figure 5B). Besides, we used western blotting to analyze the expression of EMT-related proteins in cisplatin treated cell lines when transfected with miR-421. As a

result, the expression of N-cadherin, Fibronectin, Vimentin, Snail, Slug, Twist, MMP-9 and MMP-2 was decreased by cisplatin. However, the decreased expression of N-cadherin, Fibronectin, Vimentin, Snail, Slug, Twist, MMP-9 and MMP-2 were attenuated by transfection of miR-421 in both cell lines (Figure 5C). Additionally, we also found that CoCl_2 induced high level of N-cadherin, Fibronectin, Vimentin, Snail, Slug, Twist, MMP-9 and MMP-2 could be reversed by transfection of miR-421-Inh (Figure 5C). Furthermore, we also use immunofluorescence staining to evaluate the effect of miR-421 on EMT-related proteins in gastric cancer cell. We found that miR-421 increased the expression of mesenchymal biomarkers N-cadherin, Fibronectin, and Vimentin compared to negative control (NC) (Figure 5D).

To further confirm the function of miR-421 in gastric cancer, the growth rate of SGC-7901 gastric cancer cell with or without antagomiR-421 was calculated after subcutaneous implantation into male BALB/c-nude mice (4 weeks old). As a result, overexpression of antagomiR-421

retarded the growth of tumor *in vivo* (Figure 5E). IHC staining illustrated that tumor derived from antagmiR-421 gastric cancer cells showed higher expression level of activated caspase-3 and lower expression level of Ki-67 compared with the control group (Figure 5E).

In the other hand, cisplatin sensitivity was evaluated *in vivo* with HGC-27 gastric cancer cell, which exhibited moderate basic expression level of miR-421. HGC-27/NC or HGC-27/miR-421 cells were subcutaneous implanted into male BALB/c-nude mice (4 weeks old). Cisplatin (5 mg/kg body weight) or PBS was intraperitoneally injected every 3 days for 4 times. Cisplatin inhibited the growth in both HGC-27/NC and HGC-27/miR-421 groups, and a much more significant reduction of the volume in HGC-27/NC group was observed. The size of PBS treated HGC-27/NC was significantly smaller than that of HGC-27/miR-421, which was consistent with that of SGC-7901 *in vivo*. Furthermore, the growth of HGC-27/miR-421 was faster

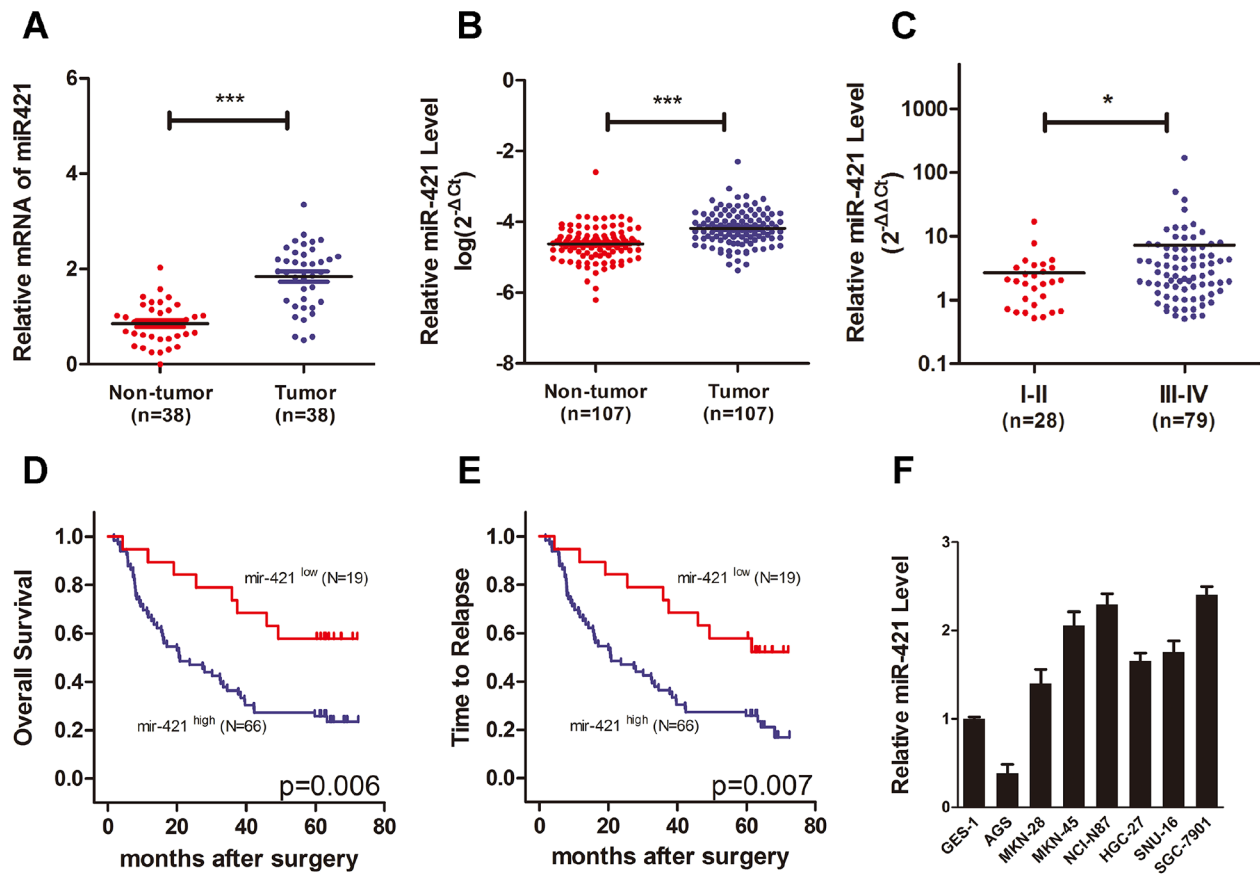


Figure 4: MiR-421 is increased in gastric cancer and associated with poor prognosis. A. Scatter dot plots show relative mRNA expression of miR-421 is significantly increased in gastric cancer tumor tissues compared with non-tumor tissues using data from The Cancer Genome Atlas. B. Scatter dot plots illustrate that the expression of miR-421 is significantly increased in tumor tissues compared with non-tumor ones in a cohort of gastric cancer specimens (n=107). C. The expression of miR-421 is higher in advanced gastric cancers compared with localized ones. D, E. Kaplan–Meier analysis illustrates that the gastric cancer patients with low levels of miR-421 have a much longer OS and TTR. F. QRT-PCR shows relative expression of miR-421 in gastric cancer cell lines (AGS, MKN-28, MKN-45, NCI-N87, HGC-27, SNU-16, and SGC-7901) compared to the immortalized human gastric epithelial cell line GES-1. Columns mean of three independent experiments. OS, overall survival; TTR, time to relapse; * $P < 0.05$; *** $P < 0.001$.

Table 1: Clinical characteristics of the gastric cancer patients

| | Expression of miR-421 | | | | P value |
|------------------------------|-----------------------|------|-----------------|------|---------|
| | Low | | High | | |
| | No. of patients | % | No. of patients | % | |
| Total | 20 | | 87 | | |
| Age | | | | | 0.394 |
| ≤ 60 | 12 | 60.0 | 43 | 49.4 | |
| > 60 | 8 | 40.0 | 44 | 50.6 | |
| Gender | | | | | 0.563 |
| Male | 17 | 85.0 | 69 | 79.3 | |
| Female | 3 | 15.0 | 18 | 20.7 | |
| Tumor differentiation | | | | | 0.627 |
| Undifferentiation | 0 | 0 | 2 | 2.3 | |
| Poor | 15 | 75.0 | 53 | 60.9 | |
| Moderate | 5 | 15.0 | 31 | 35.7 | |
| Well | 0 | 0 | 1 | 1.1 | |
| Tumor stage | | | | | 0.150 |
| I-II | 8 | 40.0 | 21 | 24.1 | |
| III-IV | 12 | 60.0 | 66 | 75.9 | |
| Tumor site | | | | | 0.512 |
| Cardia | 3 | 15.0 | 25 | 28.8 | |
| Fundus | 1 | 5.0 | 1 | 1.1 | |
| Body | 10 | 50.0 | 36 | 41.4 | |
| Antrum | 6 | 30.0 | 23 | 26.4 | |
| Pylorus | 0 | 0 | 2 | 2.3 | |
| Vascular invasion | | | | | 0.735 |
| Yes | 13 | 65.0 | 53 | 60.9 | |
| No | 7 | 35.0 | 34 | 39.1 | |
| Nerve invasion | | | | | 0.175 |
| Yes | 10 | 50.0 | 48 | 55.2 | |
| No | 10 | 50.0 | 39 | 44.8 | |

than that of HGC-27/NC when treated with cisplatin, which suggested that miR-421 contributed to cisplatin resistance. These results indicated that overexpression of miR-421 promoted that tumor malignant behavior of gastric cancer.

E-cadherin and caspase-3 are targets of miR-421

To identify the potential downstream target of miR-421, TargetScan (<http://www.targetscan.org>), miRanda (<http://www.microrna.org/microrna/hpme.do>), and miRWalk (<http://www.umm.uni-heidelberg.de/apps/>

zmf/mirwalk) online databases were used for analysis. Considering the candidate target genes predicted by the three online databases and function of miR-421, E-cadherin and caspase-3 were chose as candidate targets of miR-421. Previous researches reported that E-cadherin and caspase-3 were key regulators in the process of EMT and apoptosis, respectively, and loss function of E-cadherin and caspase-3 were common phenomena in cancer development.

To identify whether E-cadherin and caspase-3 were down regulated after the transfection of miR-421, SGC-7901 and AGS cells were transfected with miR-421 for 48h, and

Table 2: Univariate and multivariate analyses of predictors of overall survival and time to relapse in gastric cancer patients

| Variables | Overall Survival | | | | | | | Time to Relapse | | | | | | | | |
|------------------------------|------------------|----|----|------|-----------------------|---------------------|-----------------------|-----------------|----|----|----------------------|-----------------------|---------------------|------------------------|--|--|
| | Death | | | | Univariable analysis | | | Recurrence | | | Univariable analysis | | | Multivariable analysis | | |
| | Yes | No | N | % | <i>P</i> ^a | HR (95% CI) | <i>P</i> ^b | Yes | No | N | % | <i>P</i> ^a | HR (95% CI) | <i>P</i> ^b | | |
| Age | | | | | | | | | | | | | | | | |
| ≤ 60 | 28 | 15 | 43 | 50.6 | 0.681 | | | 29 | 14 | 43 | 50.6 | 0.748 | | | | |
| > 60 | 30 | 12 | 42 | 49.4 | | | | 32 | 10 | 42 | 49.4 | | | | | |
| Gender | | | | | | | | | | | | | | | | |
| Male | 48 | 21 | 69 | 81.2 | 0.489 | | | 51 | 18 | 69 | 81.2 | 0.367 | | | | |
| Female | 10 | 6 | 16 | 18.8 | | | | 10 | 6 | 16 | 18.8 | | | | | |
| Tumor differentiation | | | | | | | | | | | | | | | | |
| Undifferentiated/Poor | 40 | 15 | 55 | 64.7 | 0.083 | | | 42 | 13 | 55 | 64.7 | 0.079 | | | | |
| Moderate/Well | 18 | 12 | 30 | 35.3 | | | | 19 | 11 | 30 | 35.3 | | | | | |
| Vascular invasion | | | | | | | | | | | | | | | | |
| Yes | 40 | 13 | 53 | 62.4 | 0.048 | 0.868 (0.456-1.655) | 0.667 | 42 | 11 | 53 | 62.4 | 0.052 | | | | |
| No | 18 | 14 | 32 | 37.6 | | | | 19 | 13 | 32 | 37.6 | | | | | |
| Nerve invasion | | | | | | | | | | | | | | | | |
| Yes | 42 | 6 | 48 | 56.5 | 0.000 | 2.919 (1.464-5.821) | 0.002 | 43 | 5 | 48 | 56.5 | 0.000 | 2.576 (1.446-4.590) | 0.001 | | |
| No | 16 | 21 | 37 | 43.5 | | | | 18 | 19 | 37 | 43.5 | | | | | |
| Tumor stage | | | | | | | | | | | | | | | | |
| I-II | 5 | 15 | 20 | 23.5 | 0.000 | 3.800 (1.474-9.795) | 0.006 | 7 | 13 | 20 | 23.5 | 0.000 | 3.184 (1.395-7.268) | 0.006 | | |
| III-IV | 53 | 12 | 65 | 76.5 | | | | 54 | 11 | 65 | 76.5 | | | | | |
| miR-421 | | | | | | | | | | | | | | | | |
| High | 50 | 16 | 66 | 77.6 | 0.006 | 2.586 (1.194-5.599) | 0.016 | 52 | 14 | 66 | 77.6 | 0.007 | 2.465 (1.201-5.060) | 0.014 | | |
| Low | 8 | 11 | 19 | 22.4 | | | | 9 | 10 | 19 | 22.4 | | | | | |

HR, hazard risk ratio; 95%CI, 95% confidence interval.

^a Statistical analysis was conducted by Kaplan–Meier method (log-rank test).

^b Cox proportional hazards regression.

the protein level of E-cadherin and caspase-3 were examined. We found that the expression of E-cadherin and caspase-3 were drastically suppressed after transfection of miR-421,

indicating E-cadherin and caspase-3 were regulated by miR-421 and could be the downstream targets of miR-421 (Figure 6A).

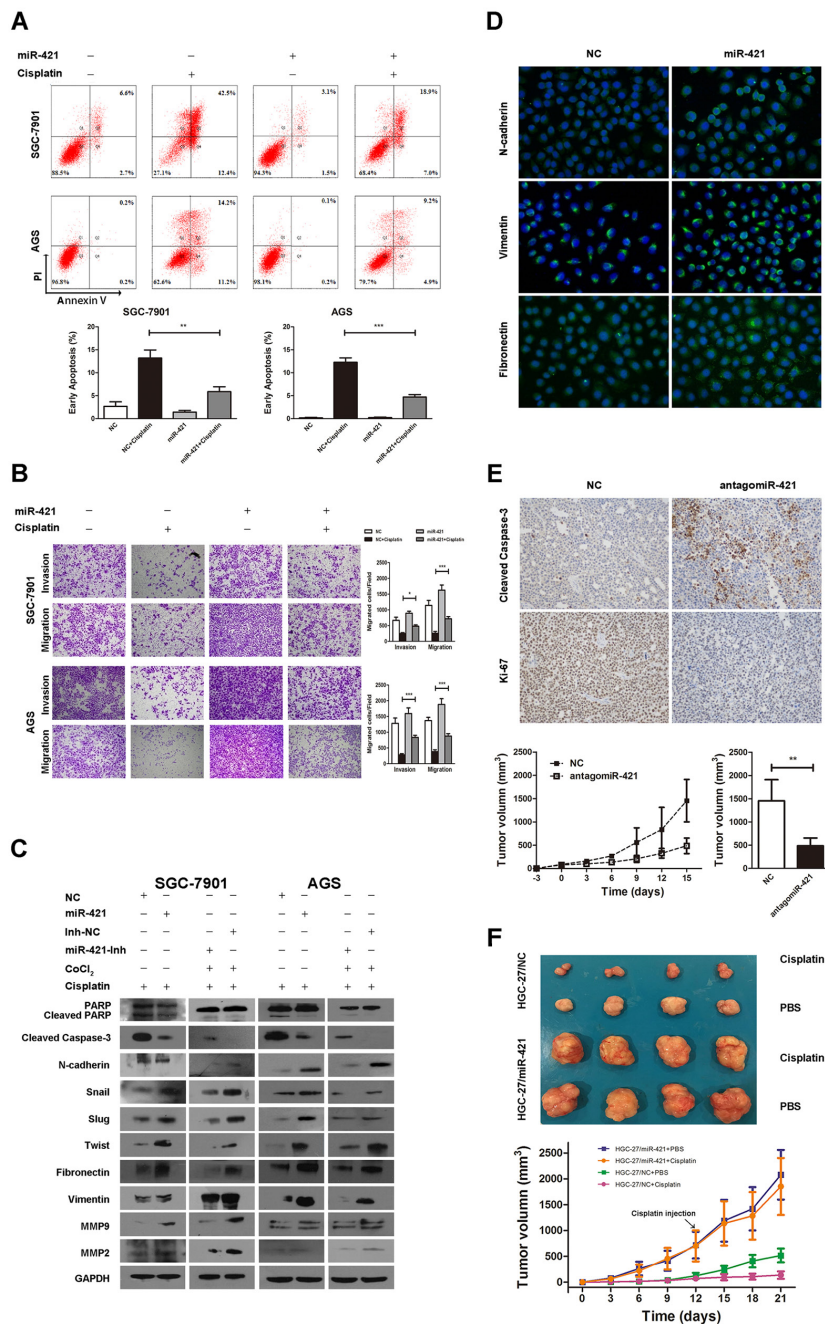


Figure 5: Overexpression of miR-421 promotes metastasis, inhibits apoptosis, and induces cisplatin resistance in gastric cancer. **A.** Flow cytometry analysis indicates that cisplatin drastically increases the percentage of early apoptotic cells in SGC-7901 and AGS cell lines, which could be attenuated by transfection of miR-421. Representative images and quantitative analysis of cell apoptosis are presented. Columns mean of three independent experiments, and bars SD. **B.** Transwell assays illustrate that cisplatin decreased the migration and invasion ability in both cell lines, and the inhibitory effect could be reversed by transfection of miR-421. Representative migration and invasion images at $\times 100$, and quantitative analysis of transwell assays are presented. Columns mean of three independent experiments, and bars SD. **C.** Western blot analysis shows that the expression of cleaved caspase-3 and cleaved PARP are induced by cisplatin, and N-cadherin, Fibronectin, Vimentin, Snail, Slug, Twist, MMP-9, and MMP-2 decreased, which could be reversed by transfection of miR-421. CoCl₂ induces low level of cleaved caspase-3 and cleaved PARP, and high level of N-cadherin, Fibronectin, Vimentin, Snail, Slug, Twist, MMP-9, and MMP-2, which could be reversed by transfection of miR-421-Inh. **D.** Immunofluorescence staining illustrates that miR-421 increased the expression of N-cadherin, Fibronectin, and Vimentin compared to NC. **E.** Overexpression of antagomiR-421 retards the growth of SGC-7901 formed tumor in vivo. IHC staining illustrates that tumor derived from antagomiR-421-overexpressed gastric cancer cells shows higher level of cleaved caspase-3 and lower level of Ki-67 compared with the control group. Error bars mean of SD. **F.** Overexpression of miR-421 promotes tumor growth and contributes to cisplatin resistance in vivo. HGC-27/NC and HGC-27/miR-421 cells were subcutaneously implanted. When palpable tumors arose, each group were randomized to be injected intraperitoneally with cisplatin (5mg/kg body weight) or PBS every 3 days. The representative tumors in the 4 groups were illustrated. Tumor volumes in the nude mice of the 4 groups were measured every 3 days. Error bars mean of SD. ** $P < 0.01$; *** $P < 0.001$.

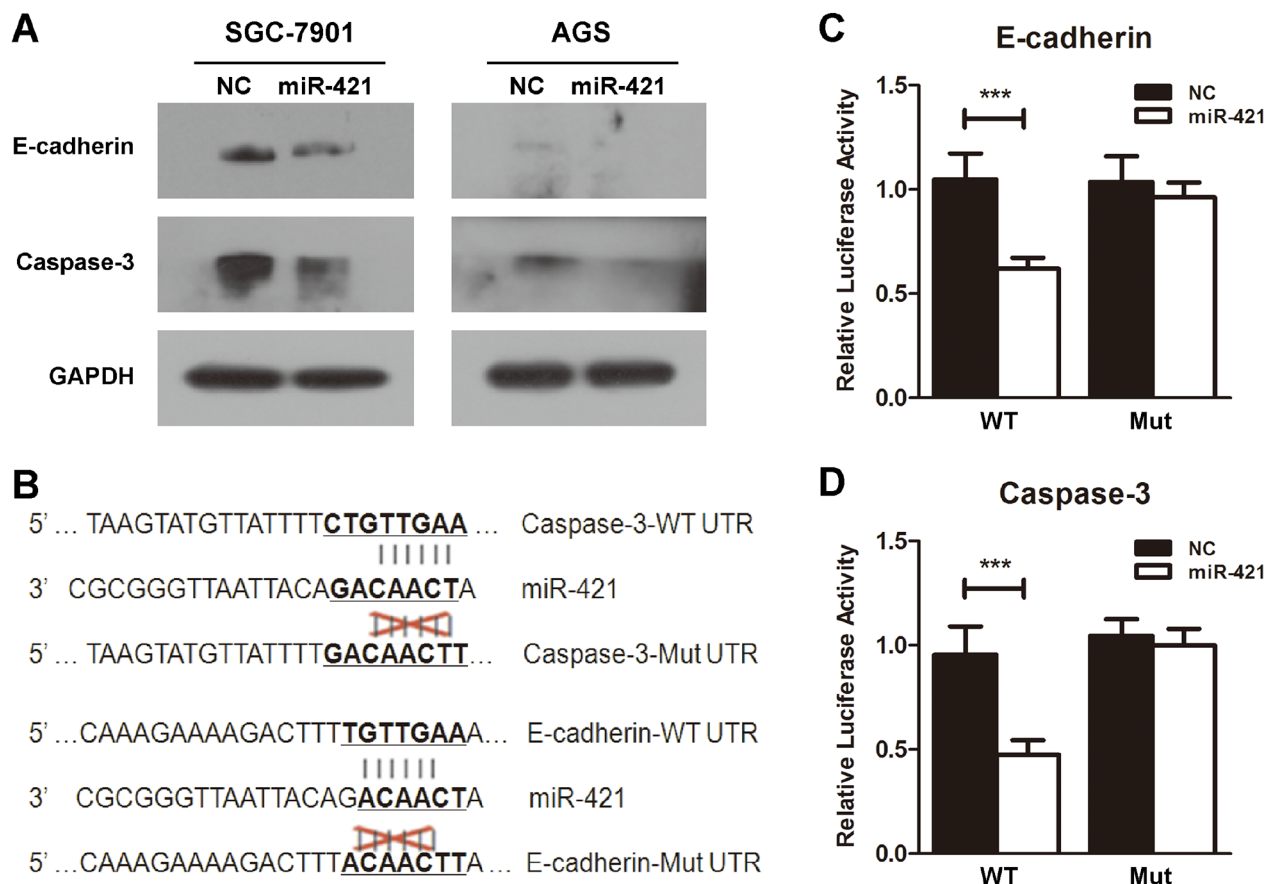


Figure 6: E-cadherin and caspase-3 are targets of miR-421. **A.** Elevated expression of E-cadherin and caspase-3 was determined by western blot when SGC-7901 and AGS cells were transfected with miR-421. **B.** Predicted miR-421 target sequences in the 3'-UTR of E-cadherin and caspase-3 are illustrated. **C.** and **D.** The HEK293T cells transfected with WT-3'-UTR of E-cadherin or caspase-3 vector and miR-421 significantly decrease the relative luciferase activity compared with transfection of WT-3'-UTR vector and NC. Co-transfection with Mut-3'-UTR vector and miR-421 or NC doesn't inhibit the relative luciferase activity. Columns mean of three independent experiments, and bars SD. *** $P < 0.001$.

To further determine whether E-cadherin and caspase-3 were direct downstream targets of miR-421, the 3'-UTR of E-cadherin and caspase-3 were synthesized and cloned into downstream of pmirGLO Dual-Luciferase miRNA Target Expression Vector with firefly luciferase. Besides, vectors with mutated binding sites of E-cadherin and caspase-3 were also constructed (Figure 6B). As a result, the HEK293T cells transfected with WT-3'UTR vector and miR-421 significantly decreased the relative luciferase activity compared with transfection of WT-3'UTR vector and NC. Nevertheless, co-transfection with Mut-3'UTR vector and miR-421 or NC didn't inhibit the relative luciferase activity (Figure 6C, 6D). These results indicated that E-cadherin and caspase-3 were the direct targets of miR-421 based on the luciferase assays.

DISCUSSION

This study illustrated that miR-421 up regulated by HIF-1 α involved in the regulation of drug resistance crosstalk with EMT promotion and apoptosis inhibition.

To determine novel drug resistance related miRNAs under hypoxic conditions, we referred to a previous published microRNA microarray (GSE 56870) and used qRT-PCR to verify the data of the microchip. As a result, we chose miR-421 as a candidate miRNA, and used *in vitro* and *in vivo* assays to identify its function in gastric cancer. Furthermore, we also found that miR-421 was an important prognostic marker in gastric cancer. Therefore, targeting miR-421/ E-cadherin/caspase-3 could be a potential strategy for the treatment of cisplatin-resistance gastric cancer patients.

EMT has been identified to be involved in the process of drug resistance in many types of tumor cells [22–27]. Platelet-derived growth factor-D (PDGF-D) pathway was involved in the acquisition of EMT characteristics of gemcitabine resistant hepatocellular carcinoma cells [22]. Induction of EMT contributed to the decreased therapeutic efficacy of oxaliplatin in colorectal cancer, due to the transition of the tumor cells from a proliferative to invasive phenotype [26]. Besides, EMT was also involved in paclitaxel and tamoxifen

resistant breast cancer cells [24, 25]. Additionally, blockade of Endothelin-1 (ET-1)/endothelin A receptor driven EMT could overcome cisplatin resistance and improve the outcome of epithelial ovarian cancer patients' treatment [27]. To the best of our knowledge, only a few reports published so far regarding the association between EMT and drug resistance of gastric cancer. Zhang et al [28] illustrated that the aggressive phenotype of adriamycin resistant gastric cancer cells was regulated by induction of EMT and activation of the canonical Wnt/ β -catenin pathway, which could be suppressed by pantoprazole which targeted the EMT and Akt/GSK-3 β / β -catenin signaling. EMT was also involved in lapatinib resistant HER2-positive gastric cancer [29]. In our study, we found that transfection of HIF-1 α -induced-miR-421 significantly down regulated the epithelial biomarker E-cadherin and up regulated N-cadherin, Fibronectin, Vimentin, Snail, Slug, Twist, MMP-2, and MMP-9 in cisplatin treated gastric cancer cell lines. Furthermore, miR-421 drastically increased the migration and invasion ability of cisplatin treated gastric cancer cell lines, indicating that miR-421-regulated EMT was involved in the process of cisplatin resistance in gastric cancer cells.

Inhibitor of miR-944 promoted cisplatin-induced apoptosis through loss of mitochondrial membrane potential and activation of caspase-3 in breast cancer [30]. Elevated HIF-1 α induced miR-424 decreased breast cancer sensitivity to doxorubicin by suppressing the expression of PDCD4, known as an apoptosis-related protein, and subsequently inhibiting the expression of caspase-3 and PARP [8]. ARC (Apoptosis Repressor with Caspase Recruitment Domain) is identified as an endogenous inhibitor of apoptosis [31] which has the unusual property of inhibiting both extrinsic and intrinsic pathways [32]. It was reported that elevated expression of endogenous ARC promoted breast carcinogenesis by inducing chemoresistance in invasive cells, and by increasing the proliferation, invasion and metastasis ability of primary tumor [33]. miR-185 was reported to increase gastric cancer sensitivity to cisplatin and doxorubicin by inhibiting the expression of ARC [34]. In our study, we found that HIF-1 α -induced miR-421 significantly attenuated the apoptotic ability induced by cisplatin, and reversed the cisplatin induced activation of caspase-3 and cleavage of PARP in gastric cancer cell lines.

Previous studies illustrated that the famous hypoxamiR, miR-210, increased cancer cell proliferation and invasion by targeting various genes [35, 36]. In our study, HIF-1 α was stabilized by CoCl₂ and bound to the HRE site of the promoter region of miR-421, subsequently increasing the expression of miR-421. Besides, transfection of Si-HIF-1 α together with induction of CoCl₂, the increased luciferase activity would be

diminished compared to induction of CoCl₂ alone. Therefore, we identified the HIF-1 α induced miR-421 as a hypoxamiR and elucidated its potential function in EMT and apoptosis related drug resistance.

miR-421 has been regarded as an onco-microRNA in neuroblastoma and hepatocellular carcinoma [19, 21]. It was reported that the N-Myc-induced miR-421 down regulated ATM (Ataxia telangiectasia-mutated gene) expression, establishing an N-Myc/miR-421/ATM pathway which contributed to N-Myc-induced carcinogenesis in neuroblastoma [37]. miR-421 induced ATM down regulation was also reported in breast cancer [38]. Moreover, miR-421 has been considered as an anti-apoptosis miRNA in nasopharyngeal carcinoma and gastric cancer [20, 39]. In our study, we observed that overexpression of miR-421 promoted tumor behavior in gastric cancer and the expression of miR-421 was significantly increased in gastric cancer tissues compared with para-cancerous tissues ($p < 0.01$) as previously reported [40]. Furthermore, for the first time, we reported that the expression of miR-421 was higher in advanced gastric cancer compared with localized gastric cancer ($p < 0.01$). Besides, those patients with low levels of miR-421 had a much longer overall survival ($p = 0.006$) and recurrence-free survival ($p = 0.007$), and miR-421 was also an independent predictor of overall survival ($p = 0.016$, HR 2.586, 95%CI 1.194-5.599) and recurrence-free survival ($p=0.014$, HR 2.465, 95%CI 1.201-5.060) by Cox multivariate analysis, indicating miR-421 could be related to cancer aggressiveness and poor prognosis.

In conclusion, our study illustrated miR-421, a HIF-1 α induced miRNA, played an important role in gastric cancer. Overexpression of miR-421 promoted metastasis, inhibited apoptosis, and induced cisplatin resistance in gastric cancer by targeting E-cadherin and caspase-3. Besides, the expression of miR-421 was detected to be higher in advanced gastric cancers compared with localized ones, and significantly increased in tumor tissues compared with non-tumor ones. Therefore, miR-421 could serve as an important prognostic marker and a potential molecular target for therapy in gastric cancer.

MATERIALS AND METHODS

Cell lines and cell culture

AGS, SGC-7901, NCI-N87 and HGC-27 human gastric cancer cell lines, and HEK293T cell line were obtained from the Cell Bank of Type Culture Collection of Chinese Academy of Sciences (Shanghai, China). MKN-28, MKN-45, SNU-16 gastric cancer cell lines, and the immortalized human gastric epithelial cell line GES-1 were obtained from 3DBiopharm Biotech Co. Ltd. All cell lines were verified by short tandem repeat (STR) DNA profiling analysis. Cells were cultured in F12K (AGS) (Gibco), RPMI1640 medium (SGC-7901) (Gibco)

containing 10% heat-inactivated fetal bovine serum (Gibco), 50U/mL penicillin and 50µg/mL streptomycin in a humid atmosphere at 37°C with 5% CO₂.

RNA isolation and real-time PCR

Expression level of miR-421 in cell lines was calculated by quantitative real-time PCR (qRT-PCR). Small RNA was extracted from cell lines with RNAiso Kit for Small RNA (TaKaRa, Japan) and subsequently reverse transcribed into cDNA with One Step PrimeScript miRNA cDNA Synthesis Kit (TaKaRa, Japan). Total RNA was extracted from cell lines with RNAiso plus (TaKaRa, Japan) and transcribed into cDNA using PrimeScript RT reagent Kit (TaKaRa, Japan). cDNAs were quantified by SYBR Premix Ex Taq (TaKaRa, Japan) by ABI 7500 fast real-time PCR System (Applied Biosystems, Carlsbad, USA). Small nuclear RNA U6 and GAPDH mRNA were used as internal controls for normalization. All primers were listed in Supplementary Table S1.

Western blotting analysis

Western blotting analysis was conducted as previously described [41]. The following primary immunoblotting antibodies were used: anti-GAPDH, anti-E-cadherin, anti-Fibronectin, anti-Vimentin, anti-Snail, anti-Slug, anti-Twist, anti-MMP-9, anti-MMP-2, anti-pro caspase-3, and anti-active caspase-3 (Epitomics, Burlingame, USA), anti-HIF-1α and anti-β-catenin (Proteintech, Chicago, USA), anti-N-cadherin (Cell Signaling Technology, Beverly, MA), and poly (ADP-ribose) polymerase (PARP) (Santa Cruz, CA).

Immunohistochemistry (IHC) staining

IHC staining was performed as previously described [42]. In short, tumor tissues from mice were dewaxed and rehydrated before conducting antigen retrieval. Slides were incubated with anti-HIF-1α (Cell Signaling Technology, Beverly, MA), anti-ki-67 or anti-active caspase-3 (Epitomics, Burlingame, USA) at 4°C overnight, followed by incubation with an HRP-conjugated secondary antibody at room temperature for 1 hour (h). Diaminobenzidine (DAB) was used for coloration, and dark brown was considered to be positive. The strength of positivity was quantified by considering the percentage of positive cells and the staining intensity.

Immunofluorescence analysis

Gastric cancer cells grown on cover slip were fixed in 4% paraformaldehyde (Invitrogen, Cergy-Pontoise, France) for 15 minutes (min). After washed three times with PBS, unspecific sites were blocked using PBS containing 5% BSA at room temperature for 1 h. Cells grown on cover slip were then incubated with anti-N-

cadherin (Cell Signaling Technology, Beverly, MA), anti-Fibronectin and anti-Vimentin (Epitomics, Burlingame, USA) at 4°C overnight, and incubated with the secondary antibodies Alexa Fluor (Molecular Probes, Life Technologies, Saint-Aubin, France) in the dark at room temperature for 1 h. DAPI were used for Nuclei staining. All stained cells were examined and photographed with a Leica SP5 confocal fluorescence microscope.

Transfection of miRNA mimics, miRNA inhibitor, antagomiRNA, small interfering RNA, and small activating RNA

miRNA-421 (miR-421), miRNA-421 inhibitor (miR-421-Inh), antagomiRNA-421 (antagomiR-421), small interfering RNA-E-cadherin (si-E-cadherin), small interfering RNA- HIF-1α (si-HIF-1α), small activating RNA-E-cadherin (ds-E-cadherin) [43] and negative control (NC) were purchased from GenePharma (Shanghai, China). Transfection was conducted via Lipofectamine 2000 (Invitrogen, Carlsbad, CA, USA) according to the manufacturer's instructions. All the small RNAs were used at a final concentration of 50nM.

Lentivirus infection

The miR-421-overexpressing lentivirus was supplied by Hanyin (Shanghai, China). HGC-27 cells were infected with the miR-421-overexpressing lentivirus (HGC-27/miR-421) or corresponding mock lentivirus (HGC-27/NC) as previously described [44]. Briefly, virus was added into the cells with 8µg/mL Polybrene® (Sigma-Aldrich, St Louis, MO, USA) for 6-8h, and then fresh culture medium was added. Forty-eight hours later, the infected cells were subjected to selection with 2µg/mL puromycin

Cell viability assay

Gastric cancer cells (4000 cells/well) were seeded into 96-well plate. After 24h incubation, the cells were treated with cisplatin (6.25-200µM) and CoCl₂ (100µM) or cisplatin alone for 48h incubation. Cell Counting Kit-8 (CCK-8, Dojindo, Kumamoto, Japan) was then added to each well after medium in it was removed and incubated for another 2h. Cell viability was measured at a solution absorbance of 450nm with MRX II absorbance reader (Dynex Technologies, Chantilly, VA, USA).

Colony formation assay

AGS and SGC-7901 gastric cancer cells were incubated for 24h after treated with cisplatin (IC₅₀) and CoCl₂/ 2'-O-Methyl modified miR-421 or cisplatin alone. Five hundreds of treated cells were then seeded into a new six-well plate and cultivated for another 14 days. Cells were subsequently fixed and stained with absolute

methanol and 0.1% crystal violet. The colony formation rate was calculated using the following equation: colony formation rate = (number of colonies/number of seeded cells) × 100%.

Cell apoptosis assay

Apoptosis was assessed by annexin V-FITC (Invitrogen, Carlsbad, CA, USA) and flow cytometry. Cells were incubated for 24h after treated with cisplatin (IC₅₀) and CoCl₂/miR-421 or cisplatin alone at a density of 1×10^6 cells in a 6-well plate. The cells were then washed twice with pre-chilled PBS, and resuspended in $1 \times$ binding buffer (1×10^6 cells/mL). Cells (100 μ L) were stained with 5 μ L annexin V-FITC and 5 μ L propidium iodide (PI) for 15 min, and 400 μ L $1 \times$ binding buffer was added. Analysis was conducted using a FC500 flow cytometer with CXP software (Beckman Coulter, Fullerton, CA, USA) within 1 h.

Transwell assay

The 24-well Boyden chamber with 8 μ m pore size polycarbonate membrane (Corning, NY) was used for evaluating the cell migration. We used Matrigel (BD, Franklin Lakes, NJ) to pre-coat the membrane to simulate a matrix barrier for evaluating the cell invasion. Forty thousand cells were seeded in the upper chamber with 150 μ L serum-free medium after treated with cisplatin (IC₅₀) and CoCl₂/miR-421 or cisplatin alone for 24h. As a chemoattractant, a total of 600 μ L medium with 10% serum was added to each lower chamber. After 24h incubation, the membranes were washed with PBS, fixed with methanol and stained with 0.1% crystal violet. We randomly selected 5 visual fields ($\times 100$) from each membrane, and the number of cells that had migrated was counted using an IX71 inverted microscope (Olympus Corp, Tokyo, Japan).

Luciferase reporter assays

The putative promoter region of miR-421 (-1 kb) harboring predicted hypoxia response element (HRE) sequences were synthesized by PCR (PrimerSTAR, TaKaRa, Japan) and cloned into pGL3 vector between SacI and NheI. CoCl₂ or DMOG treated HEK293T cells were co-transfected with cloned pGL3 vector and renilla luciferase vector with or without Si-HIF-1 α . After 48h transfection, the relative luciferase activity was calculated by Dual-Luciferase Reporter Assay System (Promega, USA).

The 3'-UTR (untranslated region) of E-cadherin and caspase-3, containing putative target region of miR-421, was synthesized (Sangon, Shanghai, China) and cloned into sites between SacI and SalI downstream of luciferase reporter gene of pmirGLO Dual-Luciferase miRNA Target Expression Vector (Promega, USA), respectively.

Additionally, the mutant miR-421 putative target region was inserted into pmirGLO Dual-Luciferase Vector in the same way. All insertions were verified by sequencing (Sangon, Shanghai, China). HEK293T cells were seeded in a 24-well plate for 24h before co-transfected with 50nM of either miR-421 or NC and 200ng reporter plasmid containing wild type (WT) or mutant type (Mut) of E-cadherin or caspase-3 3'-UTR. After 48h transfection, the relative luciferase activity was calculated by Dual-Luciferase Reporter Assay System (Promega, USA).

5-Aza-2'-deoxycytidine treatment of the AGS and SGC-7901 gastric cancer cells

AGS and SGC-7901 gastric cancer cells were treated with 10 μ L 5-Aza-2'-deoxycytidine (5-Aza) (5 μ M dissolved in DMSO) (Sigma A3656) for 4 days. RNA was extracted and analyzed for the expression of miR-421.

DNA methylation analysis

Genomic DNA from AGS and SGC-7901 gastric cancer cell lines was bisulfite modified and the CpG islands were amplified by PCR (Primers were listed in Supplementary Table S1). The PCR products were separated by agarose gel electrophoresis (3%), extracted and cloned into the pUC18 T-vector (Sangon, China). After bacterial amplification of the cloned PCR fragments by standard procedures, 10 clones were sent for DNA sequencing (Sangon, China).

Xenograft experiments

Male BALB/c-nude mice (4 weeks old) were purchased from the Shanghai Experimental Animal Center, Chinese Academy of Sciences (Shanghai, China). SGC-7901 gastric cancer cells (1×10^7 in 200 μ L PBS) were injected subcutaneously into each mouse. When palpable tumors arose, the mice in group 1 were treated with BAY 87-2243 (0.5mg/kg body weight) [45], a highly selective inhibitor of HIF-1 α , every 3 days for 15 days. The mice in group 2 were injected intratumorally with 30 μ g of Lipofectamine 2000-encapsulated antagomiR-421 or NC every 3 days for 15 days.

In the cisplatin sensitivity assays, male BALB/c-nude mice (4 weeks old) were injected subcutaneously with either HGC-27/NC or HGC-27/miR-421 cells (1×10^7 in 200 μ L PBS) [46]. Each group were randomized when palpable tumors arose, and respectively treated with intraperitoneal injection of cisplatin (5 mg/kg body weight) or PBS every 3 days [47, 48].

Tumor size was measured by 2 perpendicular diameters via caliper every 3 days. Tumor volume was calculated with the following formula $V = (\text{width}^2 \times \text{length} \times 0.52)$.

Patients and samples

A total of 107 specimens of primary gastric adenocarcinoma specimens were obtained by surgical resection between 2007 and 2010 at Fudan University Shanghai Cancer Center (Shanghai, China). All the 107 matched fresh frozen gastric adenocarcinoma tissues (C) and adjacent non-cancerous tissues (N) were selected for qRT-PCR. In order to determine the prognostic factor, follow-up was conducted, and the outcome of 85 patients was determined. Tumor staging was determined according to the tumor–node–metastasis classification system of the American Joint Committee on Cancer, 7th edition. Follow-up was performed every 6 months by specially trained staff according to standard epidemiologic procedures. Patients were acquired with informed consent, under the protocol approved by Fudan University Shanghai Cancer Center research ethics committee.

Statistical analysis

All the statistics were expressed as mean \pm standard deviation (SD) of three independent experiments. The student's t-test or One-way ANOVA was used to evaluate the between-group difference. Overall survival and recurrence-free survival were analyzed by the Kaplan–Meier method, and the log-rank test was used to estimate the differences between groups. Cox's proportional hazard model was used to assess independent prognostic indicators in the multivariate analysis. SPSS for Windows v.16.0 (SPSS, Chicago, IL) and GraphPad Prism 5.0 (GraphPad Software, La Jolla, CA) were used to conduct all the relative analyses. $P < 0.05$ was set to be statistically significant.

CONFLICTS OF INTEREST

No potential conflicts of interest were disclosed.

REFERENCES

1. Semenza GL. Oxygen sensing, hypoxia-inducible factors, and disease pathophysiology. *Annu Rev Pathol.* 2014; 9:47-71.
2. Xiao H, Tong R, Ding C, Lv Z, Du C, Peng C, Cheng S, Xie H, Zhou L, Wu J and Zheng S. gamma-H2AX promotes hepatocellular carcinoma angiogenesis via EGFR/HIF-1alpha/VEGF pathways under hypoxic condition. *Oncotarget.* 2015; 6:2180-2192. doi: 10.18632/oncotarget.2942.
3. Vaupel P. The role of hypoxia-induced factors in tumor progression. *Oncologist.* 2004; 9 5:10-17.
4. De Francesco EM, Lappano R, Santolla MF, Marsico S, Caruso A and Maggiolini M. HIF-1alpha/GPER signaling mediates the expression of VEGF induced by hypoxia in breast cancer associated fibroblasts (CAFs). *Breast Cancer Res.* 2013; 15:R64.
5. Lee HJ, Zhuang G, Cao Y, Du P, Kim HJ and Settleman J. Drug resistance via feedback activation of Stat3 in oncogene-addicted cancer cells. *Cancer Cell.* 2014; 26:207-221.
6. Singh A and Settleman J. EMT, cancer stem cells and drug resistance: an emerging axis of evil in the war on cancer. *Oncogene.* 2010; 29:4741-4751.
7. Chen D, Huang J, Zhang K, Pan B, Chen J, De W, Wang R and Chen L. MicroRNA-451 induces epithelial-mesenchymal transition in docetaxel-resistant lung adenocarcinoma cells by targeting proto-oncogene c-Myc. *Eur J Cancer.* 2014; 50:3050-3067.
8. Zhang D, Shi Z, Li M and Mi J. Hypoxia-induced miR-424 decreases tumor sensitivity to chemotherapy by inhibiting apoptosis. *Cell Death Dis.* 2014; 5:e1301.
9. Bartel DP. MicroRNAs: genomics, biogenesis, mechanism, and function. *Cell.* 2004; 116:281-297.
10. Bartel DP. MicroRNAs: target recognition and regulatory functions. *Cell.* 2009; 136:215-233.
11. Calin GA, Liu CG, Sevignani C, Ferracin M, Felli N, Dumitru CD, Shimizu M, Cimmino A, Zupo S, Dono M, Dell'Aquila ML, Alder H, Rassenti L, Kipps TJ, Bullrich F, Negrini M, et al. MicroRNA profiling reveals distinct signatures in B cell chronic lymphocytic leukemias. *Proc Natl Acad Sci U S A.* 2004; 101:11755-11760.
12. Chen X, Wang X, Ruan A, Han W, Zhao Y, Lu X, Xiao P, Shi H, Wang R, Chen L, Chen S, Du Q, Yang H and Zhang X. miR-141 is a key regulator of renal cell carcinoma proliferation and metastasis by controlling EphA2 expression. *Clin Cancer Res.* 2014; 20:2617-2630.
13. Siu MK, Abou-Kheir W, Yin JJ, Chang YS, Barrett B, Suau F, Casey O, Chen WY, Fang L, Hynes P, Hsieh YY, Liu YN, Huang J and Kelly K. Loss of EGFR signaling regulated miR-203 promotes prostate cancer bone metastasis and tyrosine kinase inhibitors resistance. *Oncotarget.* 2014; 5:3770-3784. doi: 10.18632/oncotarget.1994.
14. Rokavec M, Oner MG, Li H, Jackstadt R, Jiang L, Lodygin D, Kaller M, Horst D, Ziegler PK, Schwitalla S, Slotta-Huspenina J, Bader FG, Greten FR and Hermeking H. IL-6R/STAT3/miR-34a feedback loop promotes EMT-mediated colorectal cancer invasion and metastasis. *J Clin Invest.* 2014; 124:1853-1867.
15. Seok JK, Lee SH, Kim MJ and Lee YM. MicroRNA-382 induced by HIF-1alpha is an angiogenic miR targeting the tumor suppressor phosphatase and tensin homolog. *Nucleic Acids Res.* 2014; 42:8062-8072.
16. Kinoshita Y, Sawada K, Nakamura K, Sawada I, Toda A, Nakatsuka E, Hashimoto K, Mabuchi S, Takahashi K, Kurachi H, Lengyel E and Kimura T. The hypoxia-related microRNA miR-199a-3p displays tumor suppressor functions in ovarian carcinoma. *Oncotarget.* 2015; 6:11342-11356. doi: 10.18632/oncotarget.3604.

17. Camps C, Buffà FM, Colella S, Moore J, Sotiriou C, Sheldon H, Harris AL, Gleadle JM and Ragoussis J. hsa-miR-210 Is induced by hypoxia and is an independent prognostic factor in breast cancer. *Clin Cancer Res.* 2008; 14:1340-1348.
18. Crosby ME, Kulshreshtha R, Ivan M and Glazer PM. MicroRNA regulation of DNA repair gene expression in hypoxic stress. *Cancer Res.* 2009; 69:1221-1229.
19. Zhang Y, Gong W, Dai S, Huang G, Shen X, Gao M, Xu Z, Zeng Y and He F. Downregulation of human farnesoid X receptor by miR-421 promotes proliferation and migration of hepatocellular carcinoma cells. *Mol Cancer Res.* 2012; 10:516-522.
20. Chen L, Tang Y, Wang J, Yan Z and Xu R. miR-421 induces cell proliferation and apoptosis resistance in human nasopharyngeal carcinoma via downregulation of FOXO4. *Biochem Biophys Res Commun.* 2013; 435:745-750.
21. Li Y, Li W, Zhang JG, Li HY and Li YM. Downregulation of tumor suppressor menin by miR-421 promotes proliferation and migration of neuroblastoma. *Tumour Biol.* 2014; 35:10011-10017.
22. Wu Q, Wang R, Yang Q, Hou X, Chen S, Hou Y, Chen C, Yang Y, Miele L, Sarkar FH, Chen Y and Wang Z. Chemoresistance to gemcitabine in hepatoma cells induces epithelial-mesenchymal transition and involves activation of PDGF-D pathway. *Oncotarget.* 2013; 4:1999-2009. doi: 10.18632/oncotarget.1471.
23. Mele V, Muraro MG, Calabrese D, Pfaff D, Amatruda N, Amicarella F, Kvinlaug B, Bocelli-Tyndall C, Martin I, Resink TJ, Heberer M, Oertli D, Terracciano L, Spagnoli GC and Iezzi G. Mesenchymal stromal cells induce epithelial-to-mesenchymal transition in human colorectal cancer cells through the expression of surface-bound TGF-beta. *Int J Cancer.* 2014; 134:2583-2594.
24. Yang Q, Huang J, Wu Q, Cai Y, Zhu L, Lu X, Chen S, Chen C and Wang Z. Acquisition of epithelial-mesenchymal transition is associated with Skp2 expression in paclitaxel-resistant breast cancer cells. *Br J Cancer.* 2014; 110:1958-1967.
25. Hiscox S, Jiang WG, Obermeier K, Taylor K, Morgan L, Burmi R, Barrow D and Nicholson RI. Tamoxifen resistance in MCF7 cells promotes EMT-like behaviour and involves modulation of beta-catenin phosphorylation. *Int J Cancer.* 2006; 118:290-301.
26. Yang AD, Fan F, Camp ER, van Buren G, Liu W, Somcio R, Gray MJ, Cheng H, Hoff PM and Ellis LM. Chronic oxaliplatin resistance induces epithelial-to-mesenchymal transition in colorectal cancer cell lines. *Clin Cancer Res.* 2006; 12:4147-4153.
27. Rosano L, Cianfrocca R, Spinella F, Di Castro V, Nicotra MR, Lucidi A, Ferrandina G, Natali PG and Bagnato A. Acquisition of chemoresistance and EMT phenotype is linked with activation of the endothelin A receptor pathway in ovarian carcinoma cells. *Clin Cancer Res.* 2011; 17:2350-2360.
28. Zhang B, Yang Y, Shi X, Liao W, Chen M, Cheng AS, Yan H, Fang C, Zhang S, Xu G, Shen S, Huang S, Chen G, Lv Y, Ling T, Zhang X, et al. Proton pump inhibitor pantoprazole abrogates adriamycin-resistant gastric cancer cell invasiveness via suppression of Akt/GSK-beta/beta-catenin signaling and epithelial-mesenchymal transition. *Cancer Lett.* 2015; 356:704-712.
29. Kim HP, Han SW, Song SH, Jeong EG, Lee MY, Hwang D, Im SA, Bang YJ and Kim TY. Testican-1-mediated epithelial-mesenchymal transition signaling confers acquired resistance to lapatinib in HER2-positive gastric cancer. *Oncogene.* 2014; 33:3334-3341.
30. He H, Tian W, Chen H and Jiang K. MiR-944 functions as a novel oncogene and regulates the chemoresistance in breast cancer. *Tumour Biol.* 2015.
31. Koseki T, Inohara N, Chen S and Nunez G. ARC, an inhibitor of apoptosis expressed in skeletal muscle and heart that interacts selectively with caspases. *Proc Natl Acad Sci U S A.* 1998; 95:5156-5160.
32. Nam YJ, Mani K, Ashton AW, Peng CF, Krishnamurthy B, Hayakawa Y, Lee P, Korsmeyer SJ and Kitsis RN. Inhibition of both the extrinsic and intrinsic death pathways through nonhomotypic death-fold interactions. *Mol Cell.* 2004; 15:901-912.
33. Medina-Ramirez CM, Goswami S, Smirnova T, Bamira D, Benson B, Ferrick N, Segall J, Pollard JW and Kitsis RN. Apoptosis inhibitor ARC promotes breast tumorigenesis, metastasis, and chemoresistance. *Cancer Res.* 2011; 71:7705-7715.
34. Li Q, Wang JX, He YQ, Feng C, Zhang XJ, Sheng JQ and Li PF. MicroRNA-185 regulates chemotherapeutic sensitivity in gastric cancer by targeting apoptosis repressor with caspase recruitment domain. *Cell Death Dis.* 2014; 5:e1197.
35. Qin Q, Furong W and Baosheng L. Multiple functions of hypoxia-regulated miR-210 in cancer. *J Exp Clin Cancer Res.* 2014; 33:50.
36. McCormick RI, Blick C, Ragoussis J, Schoedel J, Mole DR, Young AC, Selby PJ, Banks RE and Harris AL. miR-210 is a target of hypoxia-inducible factors 1 and 2 in renal cancer, regulates ISCU and correlates with good prognosis. *Br J Cancer.* 2013; 108:1133-1142.
37. Hu H, Du L, Nagabayashi G, Seeger RC and Gatti RA. ATM is down-regulated by N-Myc-regulated microRNA-421. *Proc Natl Acad Sci U S A.* 2010; 107:1506-1511.
38. Bueno RC, Canevari RA, Villacis RA, Domingues MA, Caldeira JR, Rocha RM, Drigo SA and Rogatto SR. ATM down-regulation is associated with poor prognosis in sporadic breast carcinomas. *Ann Oncol.* 2014; 25:69-75.
39. Wu JH, Yao YL, Gu T, Wang ZY, Pu XY, Sun WW, Zhang X, Jiang YB and Wang JJ. MiR-421 regulates apoptosis of BGC-823 gastric cancer cells by targeting caspase-3. *Asian Pac J Cancer Prev.* 2014; 15:5463-5468.

40. Wu J, Li G, Yao Y, Wang Z, Sun W and Wang J. MicroRNA-421 is a new potential diagnosis biomarker with higher sensitivity and specificity than carcinoembryonic antigen and cancer antigen 125 in gastric cancer. *Biomarkers*. 2015; 20:58-63.
41. Wang X, Wu J, Lin Y, Zhu Y, Xu X, Liang Z, Li S, Hu Z, Zheng X and Xie L. MicroRNA-320c inhibits tumorous behaviors of bladder cancer by targeting Cyclin-dependent kinase 6. *J Exp Clin Cancer Res*. 2014; 33:69.
42. Chen H, Lin YW, Mao YQ, Wu J, Liu YF, Zheng XY and Xie LP. MicroRNA-449a acts as a tumor suppressor in human bladder cancer through the regulation of pocket proteins. *Cancer Lett*. 2012; 320:40-47.
43. Mao Q, Li Y, Zheng X, Yang K, Shen H, Qin J, Bai Y, Kong D, Jia X and Xie L. Up-regulation of E-cadherin by small activating RNA inhibits cell invasion and migration in 5637 human bladder cancer cells. *Biochem Biophys Res Commun*. 2008; 375:566-570.
44. Dai C, Lin F, Geng R, Ge X, Tang W, Chang J, Wu Z, Liu X, Lin Y, Zhang Z and Li J. Implication of combined PD-L1/PD-1 blockade with cytokine-induced killer cells as a synergistic immunotherapy for gastrointestinal cancer. *Oncotarget*. 2016. doi: 10.18632/oncotarget.7243.
45. Ellinghaus P, Heisler I, Unterschemmann K, Haerter M, Beck H, Greschat S, Ehrmann A, Summer H, Flamme I, Oehme F, Thierauch K, Michels M, Hess-Stumpp H and Ziegelbauer K. BAY 87-2243, a highly potent and selective inhibitor of hypoxia-induced gene activation has antitumor activities by inhibition of mitochondrial complex I. *Cancer Med*. 2013; 2:611-624.
46. Liu X, Ge X, Zhang Z, Zhang X, Chang J, Wu Z, Tang W, Gan L, Sun M and Li J. MicroRNA-940 promotes tumor cell invasion and metastasis by downregulating ZNF24 in gastric cancer. *Oncotarget*. 2015; 6:25418-25428. doi: 10.18632/oncotarget.4456.
47. Cho HJ, Kim IK, Park SM, Baek KE, Nam IK, Park SH, Ryu KJ, Choi J, Ryu J, Hong SC, Jeong SH, Lee YJ, Ko GH, Kim J, Won Lee C, Soo Kang S, et al. VEGF-C mediates RhoGDI2-induced gastric cancer cell metastasis and cisplatin resistance. *Int J Cancer*. 2014; 135:1553-1563.
48. Tang X, Hu G, Xu C, Ouyang K, Fang W, Huang W, Zhang J, Li F, Wang K, Qin X and Li Y. HZ08 reverse the aneuploidy-induced cisplatin-resistance in Gastric cancer by modulating the p53 pathway. *Eur J Pharmacol*. 2013; 720:84-97.